

2008

# Interface-Induced Spin and Dipole Ordering of the Copper Spin $\frac{1}{2}$ Molecule: Bis(4-cyano-2,2,6,6-tetramethyl-3,5-heptanedionato)copper(II)

David Wisbey  
*University of Nebraska - Lincoln*

Ning Wu  
*University of Nebraska - Lincoln*

Danqin Feng  
*University of Nebraska - Lincoln*

Anthony N. Caruso  
*North Dakota State University, anthony.caruso@ndsu.edu*

John Belot

*See next page for additional authors*

Follow this and additional works at: <http://digitalcommons.unl.edu/physicsdowben>

 Part of the [Physics Commons](#)

---

Wisbey, David; Wu, Ning; Feng, Danqin; Caruso, Anthony N.; Belot, John; Losovyj, Yaroslav B.; Vescovo, Elio; and Dowben, Peter A., "Interface-Induced Spin and Dipole Ordering of the Copper Spin  $\frac{1}{2}$  Molecule: Bis(4-cyano-2,2,6,6-tetramethyl-3,5-heptanedionato)copper(II)" (2008). *Peter Dowben Publications*. 226.  
<http://digitalcommons.unl.edu/physicsdowben/226>

This Article is brought to you for free and open access by the Research Papers in Physics and Astronomy at DigitalCommons@University of Nebraska - Lincoln. It has been accepted for inclusion in Peter Dowben Publications by an authorized administrator of DigitalCommons@University of Nebraska - Lincoln.

---

**Authors**

David Wisbey, Ning Wu, Danqin Feng, Anthony N. Caruso, John Belot, Yaroslav B. Losovyj, Elio Vescovo, and Peter A. Dowben

# Interface-Induced Spin and Dipole Ordering of the Copper Spin 1/2 Molecule: Bis(4-cyano-2,2,6,6-tetramethyl-3,5-heptanedionato)copper(II)

David Wisbey,<sup>†</sup> Ning Wu,<sup>†</sup> Danqin Feng,<sup>†</sup> A. N. Caruso,<sup>‡</sup> John Belot,<sup>§</sup> Yaroslav Losovyj,<sup>||</sup> Elio Vescovo,<sup>⊥</sup> and Peter A. Dowben<sup>\*,†</sup>

Department of Physics and Astronomy and the Nebraska Center for Materials and Nanoscience, University of Nebraska—Lincoln, Lincoln, Nebraska 68588-0111, Department of Physics, 257 Flarsheim Hall, University of Missouri—Kansas City, 5110 Rockhill Road, Kansas City, Kansas 64110, Department of Chemistry and the Nebraska Center for Materials and Nanoscience, University of Nebraska—Lincoln, Lincoln, Nebraska 68588-0304, Center for Advanced Microstructures & Devices, 6980 Jefferson Highway, Baton Rouge, Louisiana 70806, and National Synchrotron Light Source, Brookhaven National Laboratory, Upton, New York 11973

Received: May 13, 2008; Revised Manuscript Received: June 25, 2008

Using light-polarization-dependent angle-resolved photoemission, the metal–organic molecule bis(4-cyano-2,2,6,6-tetramethyl-3,5-heptanedionato)copper(II) (or Cu(CNdpm)<sub>2</sub>, i.e., C<sub>24</sub>H<sub>36</sub>N<sub>2</sub>O<sub>4</sub>Cu, Cu(II)) is observed to adopt a preferential orientation that depends on the film thickness and substrate when adsorbed on Co(111) and Cu(111). In addition, the final-state binding energies change with film thickness, suggesting the substrates affect the screening or charging in the photoemission final state. For Cu(CNdpm)<sub>2</sub> deposited on Co(111), the induced spin polarization was found to depend strongly on the molecular orbital contributions.

## 1. Introduction

A conducting ferromagnetic substrate can contribute to both magnetic and electric dipole ordering. Conducting substrates can induce an electric dipole in a variety of large molecular adsorbate systems.<sup>1–6</sup> Among these large molecular systems are the metal center macrocyclic metal–organic complexes, including the metal phthalocyanines.<sup>6–16</sup> Similarly, ferromagnetic substrates can induce magnetic moment ordering in an adsorbate.<sup>17,18</sup> The induced magnetic ordering due to a ferromagnetic substrate can be simply understood by the Landau–Ginzburg equation.<sup>19–32</sup> This is a mean field “proximity effect”, characterized by an exponential decay of the magnetization with film thickness  $z$  as

$$M(z) = R \exp(-\kappa z) \quad (1)$$

with a temperature-dependent characteristic paramagnetic correlation length  $\kappa^{-1}$ ,<sup>31,32</sup> related to short-range magnetic order. This mean field approximation (Landau–Ginzburg) does not, however, explain the origin of the adsorbate paramagnetic correlation length or the microscopic (quantum picture) mechanisms for induced magnetic ordering in molecular adlayers.<sup>32</sup> Electric dipole ordering tends to be more amenable to microscopic modeling, but such models remain fraught with complications, as even small changes in the  $\pi$ – $\pi$  stacking can have profound effects on the intermolecular interactions and can easily overcome electric dipole ordering effects.

To understand both phenomena microscopically for large adsorbates, knowledge of the molecular packing is essential.

Large (mostly) planar metal-centered metal–organic compounds such as the metal phthalocyanines<sup>8–11,17,33–35</sup> typically adsorb coplanar with the surface, i.e., lie flat on conducting substrates, but this adsorbate orientation does not always occur.<sup>14,33,36–38</sup> Furthermore, there is a tendency to adopt a canted bonding orientation with increasing film thickness.<sup>8,17,34,39</sup> This is important because, at the ferromagnetic interface with an insulator, there are now predictions of interplay between magnetic ordering and electric dipole orientation.<sup>40,41</sup>

In a vein similar to that of the metal phthalocyanines (with a transition-metal core such as Cu, Co, Ni, or Fe), there is bis(4-cyano-2,2,6,6-tetramethyl-3,5-heptanedionato)copper(II) (or Cu(CNdpm)<sub>2</sub>). Cu(CNdpm)<sub>2</sub> has been established to be very close to a molecular spin 1/2 system,<sup>42</sup> with some small ligand contributions to the total molecular magnetic moment. Because of the established and characterized ligand contributions to the magnetic moment and the evidence for extramolecular interactions,<sup>42</sup> substrate effects could be quite significant in the case of Cu(CNdpm)<sub>2</sub>, as is indeed shown here. This species has been shown to exhibit at least some short-range intermolecular magnetic coupling<sup>42</sup> and, as such, is of considerable interest with respect to possible (extrinsic) induced magnetic ordering. In this study we explore the influence of the substrate on the electronic properties and magnetic ordering of Cu(CNdpm)<sub>2</sub> grown on Cu(111) or Co(111) in an effort to establish further the importance of the complex to substrate interfaces.

## 2. Experimental Section

Cu(CNdpm)<sub>2</sub> (i.e., C<sub>24</sub>H<sub>36</sub>N<sub>2</sub>O<sub>4</sub>Cu (Cu(II))) was synthesized as described in ref 43 and isolated as large, blue block crystals (>1 cm on an edge) that exhibit high thermal stability (>400 K), reasonable volatilities, and nearly ideal tetragonal crystal symmetry.<sup>43</sup> The solid-state structure of bis(4-cyano-2,2,6,6-tetramethyl-3,5-heptanedionato)copper(II), illustrated in the inset to Figure 1, exhibits overall molecular C<sub>2h</sub> symmetry with

\* To whom correspondence should be addressed. Phone: (402) 472-9838. Fax: (402) 472-2879. E-mail: pdowben@unl.edu.

<sup>†</sup> Department of Physics and Astronomy and the Nebraska Center for Materials and Nanoscience, University of Nebraska—Lincoln.

<sup>‡</sup> University of Missouri—Kansas City.

<sup>§</sup> Department of Chemistry and the Nebraska Center for Materials and Nanoscience, University of Nebraska—Lincoln.

<sup>||</sup> Center for Advanced Microstructures & Devices.

<sup>⊥</sup> Brookhaven National Laboratory.

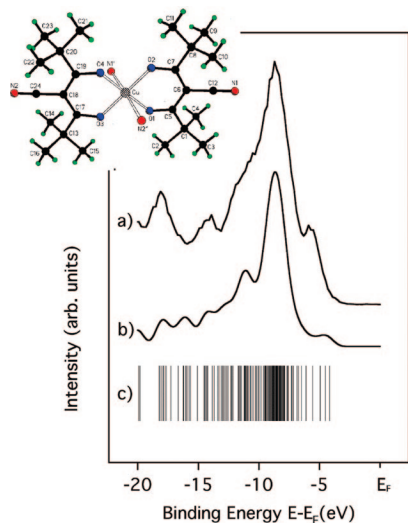


**Figure 1.** Occupied electronic structure of Cu(CNDpm)<sub>2</sub> (i.e., C<sub>24</sub>H<sub>36</sub>N<sub>2</sub>O<sub>4</sub>Cu (Cu(II))). The photoemission spectra (a) of 58 monolayers of Cu(CNDpm)<sub>2</sub> adsorbed on Co(111) at about 100 K are compared. The photoemission spectra were taken at a photon energy of 79 eV with a light incidence angle of 45° relative to the surface normal with normal emission. There is qualitative agreement with those of the calculated ground-state molecular orbitals (c) following a summation and using a 1 eV Gaussian applied to each molecular orbital after a shift of 4.4 eV in the calculated binding energies (b).

average Cu–O bond lengths of 1.92 Å.<sup>43</sup> For bulk crystals of Cu(CNDpm)<sub>2</sub>, the immediate coordination geometry about the Cu(II) metal center is a tetragonally distorted octahedron exhibiting four short Cu–O equatorial bonds and two trans axial Cu–N bonds. While the solid-state packing diagram shows independent parallel chains linked by long intermolecular Cu–NC contacts (~2.56 Å),<sup>43</sup> there is no evidence supporting the assumption that molecules adsorbed onto single crystals of Cu(111) or epitaxial Co(111) overlayers adopt a similar structure.<sup>42</sup>

Angle-resolved photoemission spectra were acquired at the U5UA undulator with a spherical grating monochromator (SGM) beamline at the National Synchrotron Light Source (NSLS)<sup>44,45</sup> and using a 3 m toroidal grating monochromator<sup>46,47</sup> at the Center for Advanced Microstructures and Devices (CAMD) in Baton Rouge, LA.<sup>48</sup> The ultra-high-vacuum photoemission end station for the SGM beamline was equipped with a commercial angle-resolved hemispherical electron energy analyzer (EA125, Omicron GmbH) and a postelectron energy analyzer Mott detector for spin polarization analysis.<sup>44,49</sup> The spin polarization  $P$  for the collected data was determined according to

$$P = \frac{1}{S} \frac{\sqrt{I_L^+ I_R^-} - \sqrt{I_L^- I_R^+}}{\sqrt{I_L^+ I_R^-} + \sqrt{I_L^- I_R^+}} \quad (2)$$

where  $I_L$  and  $I_R$  represent the number of electrons scattered into the left and right channels of the Mott detector, respectively. To eliminate instrumental asymmetry, it was necessary to measure the sample magnetized “up” ( $I_L^+$ ,  $I_R^+$ ) and the sample magnetized ‘down’ ( $I_L^-$ ,  $I_R^-$ ). Spin polarization was calculated using a Sherman function of  $S = 0.15$ . The analyzer had a  $\pm 2^\circ$  angular resolution, while the combined energy resolution of the analyzer and the light source was approximately 150 meV or less. The photoemission spectra were taken at a 45° light incidence angle, with the photoelectrons collected normal to the surface, unless indicated otherwise.

For light polarization photoemission studies that preserved the highest possible point group (preserving normal emission regardless of the light incidence angle), measurements were made in a UHV chamber employing a hemispherical electron analyzer with an angular acceptance of  $\pm 1^\circ$ , as described elsewhere<sup>46,47</sup> using plane-polarized synchrotron light dispersed by a 3 m toroidal grating monochromator.<sup>46,47</sup> The combined resolution of the electron energy analyzer and monochromator is 120–150 meV for high kinetic photon energies (50–120 eV), but higher resolution (about 80 meV) is obtained at lower photon energies of 15–40 eV. Throughout, all binding energies are referenced to the substrate Fermi level, and angles are defined with respect to the substrate surface normal.

Molecular Cu(CNDpm)<sub>2</sub> thin films were grown on surfaces of Cu(111) and Co(111). The molecule Cu(CNDpm)<sub>2</sub> was adsorbed from the vapor as described in prior work.<sup>42</sup> As with our studies of the adsorbed metallocenes,<sup>45,50</sup> the Cu(CNDpm)<sub>2</sub> molecules were deposited on the Cu(111) or Co(111) surfaces at about 100 K. Adequate Cu(CNDpm)<sub>2</sub> vapor pressure was obtained by subliming the molecule at a temperature of approximately 350 K (80 °C). Clean Cu(111) surfaces were prepared by repeated cycles of Ar<sup>+</sup> ion sputtering and annealing of a Cu single crystal. The Co(111) substrates were epitaxial cobalt films grown in situ on clean Cu(111) substrates, at room temperature, by electron-beam evaporation.<sup>42,51</sup> Cobalt substrate films were grown to a thickness of 20 Å and characterized by low-energy electron diffraction, photoemission, and spin-polarized photoemission. Typically, epitaxial Co(111) layers on Cu(111) possessed 20–40% spin polarization, depending on the incident photon energy and film thickness, consistent with the literature.<sup>52</sup> Low-energy electron diffraction (LEED) verified the clean crystalline Cu(111) and Co(111) substrates. Care was taken to avoid photodecomposition of the adsorbed molecules, as the molecule can decompose during photoemission experiments,<sup>42,53</sup> and these photodecomposition processes will be detailed elsewhere.<sup>53</sup>

### 3. Final-State Effects in Photoemission

Photoemission spectroscopy of molecular Cu(CNDpm)<sub>2</sub> films qualitatively follows expectation,<sup>42</sup> as illustrated in Figure 1, when taken at temperatures of about 100 K, where charging and final-state effects seem less significant than observed at 40 K. For several monolayer equivalent coverages of Cu(CNDpm)<sub>2</sub>, four distinct features at the same binding energies of 4–6, 8–9, 10–11, and about 14 eV emerge in the main valence occupied molecular orbitals of the molecule, while another prominent density of states is evident at a binding energy of roughly 16–18 eV. After a shift of the calculated orbital energies by about 4.4 eV (roughly the expected work function), the experiment is seen to be in qualitative agreement with a very simplistic calculated representation of the density of states based on the ground-state molecular orbitals (NDO-PM3 or neglect of differential diatomic overlap, parametric model number 3<sup>54</sup>) for a single Cu(CNDpm)<sub>2</sub> molecule, with a 1 eV width Gaussian envelope applied to each molecular orbital (the vertical lines in Figure 1c) without correction for the substrate, final-state, or matrix element effects, as has been done elsewhere.<sup>38,42,45,55,56</sup> We note the comparison of the semiempirical PM3 calculation (where the two-electron integrals are excluded), with the more accurate method—*ab initio* LCAO/LDA calculations (which contain two-electron integrals), has been seen to provide similar results for large organic systems.<sup>56</sup> Surprisingly, although ground-state calculations, the molecular orbitals so calculated are reasonably comparable to those of the final-state combined photoemission and inverse

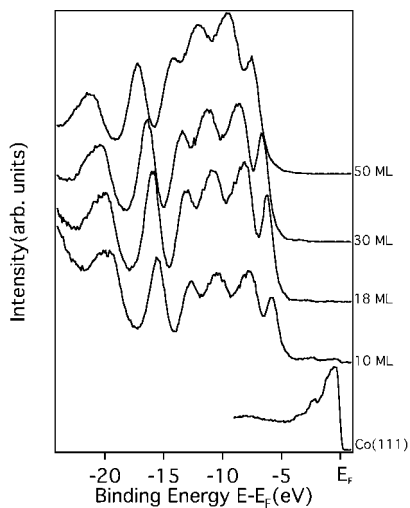


**Figure 2.** Photoemission spectra of  $\text{Cu}(\text{CNdp})_2$  deposited on  $\text{Co}(111)$  at about 40 K as a function of the molecular film thickness. The spectra were taken at a photon energy of 49 eV with a light incidence angle of  $45^\circ$  relative to the surface normal with normal emission.

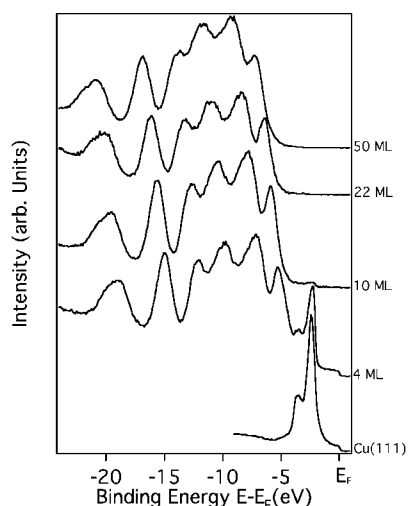


**Figure 3.** Photoemission spectra of  $\text{Cu}(\text{CNdp})_2$  deposited on  $\text{Cu}(111)$  at about 40 K as a function of increasing molecular film thickness. The spectra were taken at a photon energy of 49 eV with a light incidence angle of  $45^\circ$  relative to the surface normal with normal emission.

photoemission experimental studies. Another approach would be to use a semiempirical hybrid functional such as B3LYP.<sup>57,58</sup>

There is a strong dependence of the photoemission spectra on both the film thickness and substrate that had not been observed in prior work,<sup>42</sup> partly arising from improved energy resolution in photoemission and lower substrate temperatures. Figure 2 shows photoemission spectra of increasing molecular  $\text{Cu}(\text{CNdp})_2$  film coverages deposited on the surface of a  $\text{Co}(111)$  substrate at about 40 K. Similarly, photoemission spectra of increasing molecular  $\text{Cu}(\text{CNdp})_2$  film coverages deposited on the surface of a  $\text{Cu}(111)$  substrate at about 40 K are shown in Figure 3. With the lower photon energy of 49 eV, the photoemission features are more distinct than at 79 eV. At 79 eV, the molecular orbitals with a strong Cu weight are emphasized, due to the resonant photoemission intensity contributions from the Cu 3p core to bound-state excitations. At 49 eV, the photoemission cross-sections favor the ligand contributions, as has been noted previously.<sup>42</sup> What is observed, with the molecular films on both  $\text{Co}(111)$  (Figure 2) and  $\text{Cu}(111)$  (Figure 3) substrates at about 40 K, is an increase in

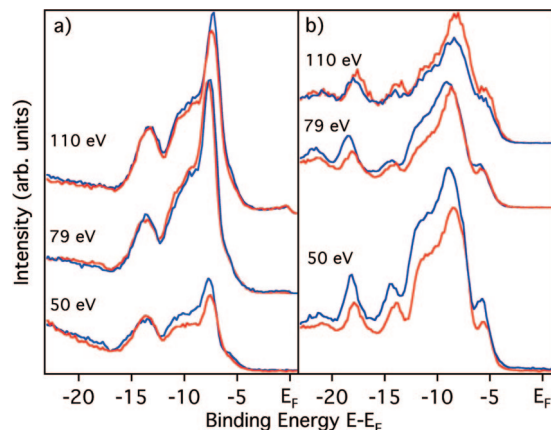


**Figure 4.** Light-polarization-dependent photoemission spectra of  $\text{Cu}(\text{CNdp})_2$  deposited on  $\text{Co}(111)$  at 100 K for a molecular film thickness of (a) 8 molecular monolayers (MLs) at the left and (b) 57 molecular MLs at the right. Data are shown for three different photon energies of 50, 79, and 110 eV for a light incidence angle of  $45^\circ$  (red) and a light incidence angle of  $70^\circ$  (blue) relative to the surface normal. All spectra were taken with electrons collected at the surface normal.

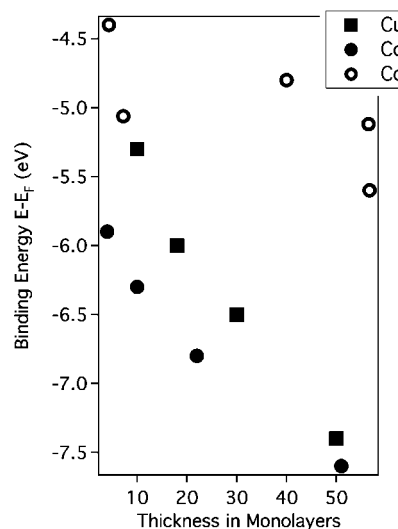


**Figure 5.** Relative change in binding energy with increasing thickness of  $\text{Cu}(\text{CNdp})_2$  molecular thin films on  $\text{Cu}(111)$  (squares) and  $\text{Co}(111)$  (solid circles) at 40 K as well as on  $\text{Co}(111)$  (open circles) at 100 K. The binding energy position of the photoemission feature attributable to the higher occupied molecular orbitals alone has been plotted. The bottom axis is the thickness of  $\text{Cu}(\text{CNdp})_2$  in molecular monolayer equivalents.

the molecular orbital derived photoemission feature binding energies, with increasing molecular film coverage. This increase in binding energy with coverage is evident but is not as dramatic with the films on the same substrates at 100 K (Figure 4 and reported in ref 42).

These increases in the binding energies of the  $\text{Cu}(\text{CNdp})_2$  features in photoemission spectra taken at about 40 and 100 K are summarized in Figure 5. The binding energy shifts of the photoemission features with coverage from the  $\text{Cu}(\text{CNdp})_2$  molecular orbitals on  $\text{Co}(111)$  and  $\text{Cu}(111)$  at about 40 K are similar with coverage, but do differ slightly between the two substrates. The binding energy difference is about 1 eV between the two substrates for the photoemission features from 10 molecular monolayers (MLs) of  $\text{Cu}(\text{CNdp})_2$ . This is much larger than variations between experiments of about 200–300 meV. At around 18 molecular MLs the difference between the

two substrates decreases to  $0.7 \pm 0.2$  eV. As the thickness reaches about 50 molecular MLs, the difference in the binding energies, for the features from the  $\text{Cu}(\text{CNdpm})_2$  molecular orbitals, is reduced to around  $0.4 \pm 0.2$  eV, as seen in Figure 5.

The changes in the binding energies with the molecular thin film thickness can arise from several sources, such as final-state effects, photohole screening, charge transfer, and changes in the molecular orientation.<sup>59–62</sup> We can distinguish between initial-state “chemical effects” and final-state effects<sup>59</sup> by investigating how the molecular orbital binding energies change with coverage and temperature. With initial-state chemical effects, which include charge transfer from the substrate,<sup>6,7,63</sup> both the highest occupied molecular orbital and lowest unoccupied molecular orbital shift relative to the substrate Fermi level in a like manner with the molecular film thickness. With final-state effects,<sup>59,60,64,65</sup> the highest occupied molecular orbital (HOMO) and lowest unoccupied molecular orbital (LUMO) gap changes, with both the HOMO and the LUMO shifting toward or away from the Fermi level in concert. While it is clear that a definitive distinction between chemical shifts and final-state effects requires combined photoemission and inverse photoemission studies<sup>59</sup> or scanning tunnel spectroscopy,<sup>66</sup> initial-state chemical shifts, based on the interface dipole, largely occur only for the first 3–5 molecular layers for molecules such as the metal phthalocyanines<sup>6,63</sup> and  $\text{C}_{60}$ <sup>66</sup> and would tend to be largely independent of temperature. In the case of  $\text{Cu}(\text{CNdpm})_2$ , the binding energy shifts in the photoemission spectra continue to persist at much higher molecular coverages and are temperature-dependent (there is a difference between 40 and 100 K in the coverage dependence of the photoemission spectra).

While both charging and screening could contribute to final-state effects, and both are consistent with the strong temperature dependence observed in the binding energy shifts with thickness, it should be noted that line shape effects expected to accompany final-state effects<sup>61,62</sup> are often not observed with molecules and are not observed here in a very pronounced fashion. The fact that final-state effects are observed, whatever their origin (including possible molecular film surface charging), tends to implicate differences in the preferential orientation of the molecules. The differences in molecular orientation are indeed seen to be substrate-dependent and affect the molecular packing for molecular films to significant thickness, as discussed below. The changing molecular orientation provides a complication that cannot be ignored.<sup>8,36,37</sup> The molecular orientation can affect not only molecular orbital alignment with respect to the substrate Fermi level (a temperature-independent effect) but also the effective dielectric properties, which could show a strong temperature dependence in photoemission.

One should note that the molecular orientation will sometimes strongly depend on the temperature<sup>67,68</sup> and the film growth temperature<sup>69</sup> so that the bonding orientation can affect intermolecular interactions, in particular the  $\pi$ – $\pi$  stacking interactions.<sup>69</sup> Such a temperature dependence of the preferential orientation will certainly contribute a small initial-state chemical shift but will profoundly enhance or suppress final-state charging and screening, by strongly affecting the hopping conductivity through the molecular film. In general, final-state effects due to charge mobility tend to be far larger than charging effects due to changing molecular orientation,<sup>68</sup> though separation of the origins of the final-state charging and screening can be very difficult in organic systems.

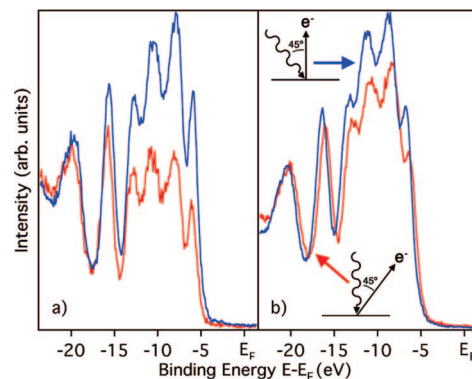


**Figure 6.** Light-polarization-dependent photoemission spectra of  $\text{Cu}(\text{CNdpm})_2$  deposited on  $\text{Cu}(111)$  at 40 K with a fixed angle between the light incidence and electron emission. The spectra are shown for a  $\text{Cu}(\text{CNdpm})_2$  molecular thin film of 22 molecular MLs at the left (a) and for a thickness of 50 molecular MLs at the right (b). Spectra were taken for a light incidence angle with the electric vector in the plane of the surface and electrons collected at  $45^\circ$  relative to the surface normal (red) and for a light incidence angle of  $45^\circ$  with electrons collected along the surface normal (blue), at a photon energy of 49 eV. The insets indicate the geometry of the experiments.

#### 4. Evidence for Preferential Molecular Orientation

Light-polarization-dependent angle-resolved photoemission does provide some evidence of a preferential molecular orientation for adsorbed  $\text{Cu}(\text{CNdpm})_2$ . The plane-polarized synchrotron light, dispersed through the monochromator, provides symmetry selection rules according to<sup>70</sup>

$$\left(\frac{d\sigma}{d\Omega}\right)_{\text{PES}} = |\langle \Psi_f | \vec{A} \cdot \vec{P} + \vec{P} \cdot \vec{A} | \Psi_i \rangle|^2 \delta(E_f - E_i - h\nu) \quad (3)$$

where  $\vec{A}$  is the vector potential of the incident photon,  $\vec{P}$  is the momentum operator,  $\vec{A} \cdot \vec{P}$  is the effective dipole operator,  $\Psi_i$  and  $\Psi_f$  are the initial and final states, respectively, and  $E_i$  and  $E_f$  are initial and final energies of the electron, respectively. If the molecule truly is randomly orientated with respect to the surface normal, or canted uniformly neither in the plane of the surface nor along the surface normal (but say at  $45^\circ$  between those two orientations), then there should be no change in the photoemission intensities with light incident angle in the geometry of our experiments. In fact, for  $\text{Cu}(\text{CNdpm})_2$  adsorbed on  $\text{Cu}(111)$ , there is a profound difference in photoemission spectra taken with larger light incidence angles and light vector potential oriented more along the surface normal (blue spectra in Figure 4), as compared to small light incidence angles and light vector potential oriented more along the surface plane (red spectra in Figure 4).

The coverage dependence of the preferential orientation for  $\text{Cu}(\text{CNdpm})_2$  differs when deposited on either  $\text{Co}(111)$  or  $\text{Cu}(111)$ . This suggests differences in the  $\text{Cu}(\text{CNdpm})_2$  interaction with  $\text{Co}(111)$  and  $\text{Cu}(111)$ . Although less easy to interpret when both the light incidence and photoelectron emission angles change, the differences in preferential orientation for  $\text{Cu}(\text{CNdpm})_2$  on  $\text{Co}(111)$  and  $\text{Cu}(111)$  are evident when Figures 6 and 7 are compared.

Like those of copper phthalocyanine,<sup>39</sup> the molecular orbitals of  $\text{Cu}(\text{CNdpm})_2$  are generally enhanced with a light polarization placing the vector potential increasingly oriented along the surface normal (Figures 4, 6, and 7). We may conclude that  $\text{Cu}(\text{CNdpm})_2$ , on the basis of symmetry selection rules in photoemission and inspection of the various molecular orbital contributions to each of the photoemission features, tends to adopt a preferential orientation so that the complex lies largely coplanar with the substrate interface.

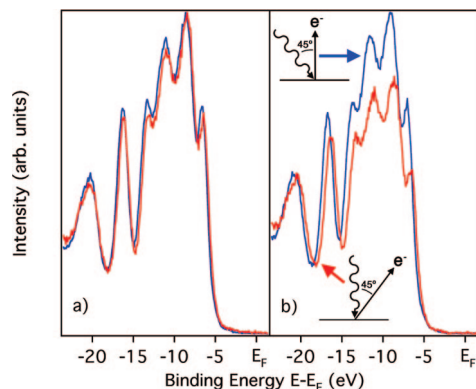


**Figure 7.** Light-polarization-dependent photoemission spectra of  $\text{Cu}(\text{CNdp})_2$  deposited on  $\text{Co}(111)$  at 40 K with a fixed angle between the light incidence and electron emission. The spectra are shown for a  $\text{Cu}(\text{CNdp})_2$  molecular thin film of 30 molecular MLs at the left (a) and for a thickness of 50 molecular MLs at the right (b). Spectra were taken for a light incidence angle with the electric vector in the plane of the surface and electrons collected at  $45^\circ$  relative to the surface normal (red) and for a light incidence angle of  $45^\circ$  with electrons collected along the surface normal (blue), at a photon energy of 49 eV. The insets indicate the geometry of the experiments.

Surprisingly, this preferential planar orientation is adopted only with increasing molecular film thickness on  $\text{Co}(111)$ . This molecular orientation adopted for the thicker molecular  $\text{Cu}(\text{CNdp})_2$  films on  $\text{Co}(111)$  is evident from the greater light polarization dependence in photoemission. This suggests either that the preferential orientation of  $\text{Cu}(\text{CNdp})_2$  at the  $\text{Co}(111)$  interface is canted or that at the  $\text{Co}(111)$  interface the molecule is in a configuration far from planar. The latter nonplanar molecular configuration must be considered as this occurs in the bulk  $\text{Cu}(\text{CNdp})_2$  crystals.<sup>42,43</sup> With increasing molecular film thickness on  $\text{Co}(111)$ , the molecular  $\text{Cu}(\text{CNdp})_2$  layers adopt an increasing planar orientation with respect to the substrate surface, eventually losing preferential orientation with even greater  $\text{Cu}(\text{CNdp})_2$  film thickness on  $\text{Co}(111)$ . By way of comparison, on some substrates copper phthalocyanine is also canted or “upright”,<sup>33,36</sup> as is possibly adsorbed (5,7,12,14-tetramethyl-2,3:9,10-dibenzo[*b,i*]-1,4,8,11-tetraazacyclotetradecine)cobalt(II) ( $\text{Co}^{\text{II}}\text{TMTAA}$ ) on  $\text{Au}(111)$ , although the latter system may also be in a nonplanar (saddle-shaped) molecular configuration.<sup>38</sup>

In any case, the molecular packing of  $\text{Cu}(\text{CNdp})_2$  on  $\text{Cu}(111)$  and  $\text{Co}(111)$  differs substantially from that of the bulk molecular crystal.<sup>42,43</sup> The bulk molecular packing would provide little or no light polarization dependence in photoemission. A preferential molecular orientation so different from that observed in bulk crystals of  $\text{Cu}(\text{CNdp})_2$  suggests that at least some  $\pi$ - $\pi$  interactions exist between molecules, in the thin film limit, particularly on  $\text{Cu}(111)$ . The fact that  $\text{Cu}(\text{CNdp})_2$  adopts a more planar configuration at all suggests that even very weak molecule-substrate interactions can lead to a change in the molecular conformation, as has been observed for (5,7,12,14-tetramethyl-2,3:9,10-dibenzo[*b,i*]-1,4,8,11-tetraazacyclotetradecine)nickel(II) ( $\text{Ni}^{\text{II}}\text{TMTAA}$ ),<sup>38</sup> and cobalt(II) tetraphenylporphyrin.<sup>40</sup> With increasing  $\text{Cu}(\text{CNdp})_2$  film thickness on  $\text{Cu}(111)$ , as in the case of the metal phthalocyanines,<sup>8,17,34</sup> the preferential planar configuration is slowly lost, as indicated by the diminishing light polarization dependence in photoemission. Again a similar effect has been observed in the light-polarization-dependent photoemission for copper phthalocyanine on graphite<sup>39</sup> and other metal phthalocyanines.<sup>17,34</sup>

The likely  $\pi$ - $\pi$  interactions that accompany a preferential bonding orientation do suggest that the substrate does affect

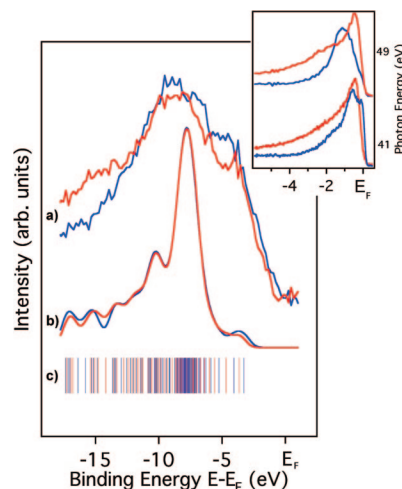


**Figure 8.** Spin-polarized photoemission of about 10 molecular MLs of  $\text{Cu}(\text{CNdp})_2$  deposited on  $\text{Co}(111)$  at  $T \approx 40$  K at a thickness of about 30 Å. The spectra were taken at a normal emission angle with a light incident angle of  $45^\circ$  relative to the surface normal and a photon energy of 49 eV. The spin-polarized photoemission spectra (a) are compared with those of the calculated spin ground-state molecular orbitals (c) following a summation and using a 1 eV Gaussian applied to each molecular orbital after a shift of 4.4 eV in calculated binding (b). Red indicates the spin majority while blue indicates the spin minority throughout. The inset shows the spin-polarized photoemission spectra for clean  $\text{Co}(111)$  grown on  $\text{Cu}(111)$  for two photon energies but an otherwise similar photoemission geometry.

the molecular orientation. In general, the metal phthalocyanines, metal tetraazaannulenes, and many metal porphyrins, such as  $\text{Cu}(\text{CNdp})_2$ , are not perfect planar molecules. With a change in molecular orientation, there is a change in molecule dipole orientation. As suggested above, as the orientation of the molecule changes, so does the effective dipole layer, thus altering the binding energy. For copper phthalocyanine, as the molecules are deposited, they shift from a flat orientation to slightly canted. This canting increases with thickness and changes the dipole layer at the interface, causing an increase in the binding energy of the molecular orbitals. Such effects, however, would not be strongly temperature-dependent unless the adlayer orientation was seen to be strongly dependent upon temperature as has been occasionally observed with large organic adlayers.<sup>55</sup>

## 5. Substrate-Induced Net Spin Polarization

Spin-polarized photoemission data were taken at temperatures of  $\sim 40$  K at a thickness of 10 molecular MLs or less. Net spin polarization was observed in the spin-polarized photoemission of  $\text{Cu}(\text{CNdp})_2$  deposited on  $\text{Co}(111)$ , as seen in Figure 8. Figure 8a shows a clear difference in the spin majority and minority intensities for the occupied states of  $\text{Cu}(\text{CNdp})_2$  deposited on  $\text{Co}(111)$ , although the resolution and count rate have been very degraded from the spin-integrated photoemission spectra so as to avoid photofragmentation of the adsorbed  $\text{Cu}(\text{CNdp})_2$  at 40 K. In spite of the reduced resolution, we find a maximum in the absolute value of the spin asymmetry of  $-10\%$  to  $-15\%$  (favoring the minority spin polarization) at binding energies of about 2–5 eV and  $+10\%$  (majority spins) at binding energies of 14–18 eV. Although the measured spin polarization differs from the model calculations for a single spin-polarized  $\text{Cu}(\text{CNdp})_2$  molecule (Figure 8b), the overall dependence of spin polarization on the molecular orbital is expected (Figure 8c).

As observed with adsorbed metal phthalocyanines on transition ferromagnetic substrates,<sup>17,18</sup> the induced magnetic order leads to a polarization asymmetry that depends on the molecular orbital contributions. The spin asymmetries observed for  $\text{Cu}(\text{CNdpm})_2$  tend to resemble that observed with copper phthalocyanine on Fe(100), although they are of opposite sign in polarization. Copper phthalocyanine on Fe(100) exhibits a +5% asymmetry near the highest occupied molecular orbitals at about 1 eV binding energy ( $-1$  eV,  $E - E_F$ ) and a slight negative spin asymmetry at binding energies ( $-12$  eV,  $E - E_F$ ) where the C 2s contributions to the molecular orbitals are likely to be stronger.<sup>17</sup> The higher, roughly 5%, spin asymmetries near the highest occupied molecular orbitals are also observed with other metal phthalocyanines on Fe(100).<sup>18</sup> The smaller absolute values of the spin asymmetries observed for the metal phthalocyanines may differ from those of  $\text{Cu}(\text{CNdpm})_2$  on Co(111) for a variety of reasons. The paramagnetic correlation length, molecular film thickness, temperature, and substrate domain structure can all play a role in establishing the observed spin polarization, as could the different probing depths of spin-polarized photoemission reported here and spin-polarized metastable de-excitation spectroscopy (the latter being far more surface sensitive) studies of the metal phthalocyanines on Fe(100).<sup>17,18</sup> Clearly a ferromagnetic substrate can induce magnetic ordering in a molecular adsorbate, resulting in a molecular-orbital-dependent spin polarization. This is not the substrate polarization, as the signs of the spin asymmetries differ significantly from that observed for cobalt at the same binding energies (inset to Figure 8).

The negative sign of the spin polarization ( $-10\%$  to  $-15\%$ ) at the smaller binding energies, for adsorbed  $\text{Cu}(\text{CNdpm})_2$  on Co(111) at 40 K, suggests that some of the molecular Cu spin density is aligned antiparallel to the Co(111) substrate moment. It is at the smaller energies that the molecular orbitals contain a strong Cu weight. The ligand polarization, as represented at the higher binding energies, may be aligned with the Co(111) substrate moment. This is very different from the metal phthalocyanines on Fe(100) at room temperature,<sup>17,18</sup> where the sign of the polarization suggests that the central metal atom is clearly aligned parallel to the substrate moment and that the ligand may have a slight spin density component antiparallel to the substrate. One implication of this result is that, for adsorbed  $\text{Cu}(\text{CNdpm})_2$  on Co(111) at 40 K, there is possible weak antiferromagnetic coupling of the Cu central atom with respect to the substrate, beginning at the interface. This would also be very different from metallic copper on cobalt, where there can be spin minority quantum well states in copper on cobalt, but the induced Cu moment is largely parallel to the Co substrate.<sup>71</sup>

The very high values of the absolute polarizations we observe for  $\text{Cu}(\text{CNdpm})_2$  on Co(111) suggest a paramagnetic correlation length (in the context of eq 1) on the order of the thickness (about 10 molecular monolayers), since the polarization in the paramagnetic limit will not exceed the polarization of clean Co(111), or about 20–40%. Alternatively, in the molecular packing arrangement adopted on Co(111), there is a weak ferromagnetic coupling and some magnetic ordering. The latter possibility would certainly be consistent with the alignment of the Cu moments in  $\text{Cu}(\text{CNdpm})_2$  antiparallel to the substrate Co moments. While the medium of exchange in the  $\text{Cu}(\text{CNdpm})_2$  has not been identified from the measurements here or elsewhere,<sup>42</sup> a strong hybridization between the Cu 3d orbitals in  $\text{Cu}(\text{CNdpm})_2$  and the substrate could lead to a reduction in the overall spin majority population in  $\text{Cu}(\text{CNdpm})_2$

adsorbed at the interface, as occurs for Ti in barium titanate on iron<sup>72</sup> and strontium titanate on cobalt.<sup>73</sup> Clearly molecular film thickness and temperature spin-dependent polarization studies are required to elucidate the mechanism(s) of the spin ordering.

Strict physisorption on Co(111) would tend to result in a net majority polarization everywhere, with a very small Pauli-type exchange splitting, as has been observed in the case of Xe on Co(111),<sup>74</sup> and this would fall off dramatically with adlayer thickness. This is certainly not the case here.

## 6. Summary

In conclusion, we have shown that  $\text{Cu}(\text{CNdpm})_2$  adopts a preferential orientation on both Co(111) and Cu(111), although there are some differences evident between the two substrates, especially at lower coverage. We find a maximum spin asymmetry of +10% at binding energies of about 4–5 eV and  $-10\%$  at binding energies of 14–18 eV. It is clear from the data, analogous to prior work with the metal phthalocyanines on transition ferromagnetic substrates,<sup>17,18</sup> that there is overall dependence of the spin polarization on the molecular orbital. The data suggest either a paramagnetic correlation length for  $\text{Cu}(\text{CNdpm})_2$  on the order of 10 molecular monolayers or that with the molecular packing arrangement adopted by  $\text{Cu}(\text{CNdpm})_2$  on Co(111) there is weak ferromagnetic coupling and some magnetic ordering at 40 K.

Given that the surface dipole layer and surface interactions can affect the adsorbate molecular dipole and molecular structural configuration, it may be that these induced changes in structure also change the magnetic properties of the molecule. Molecules such as  $\text{Cu}(\text{CNdpm})_2$  may be possible archetypical magnetoelectric systems.<sup>75</sup>

**Acknowledgment.** This research was supported by the National Science Foundation through Grant Nos. CHE-0415421 and CHE-0650453. The CAMD is supported by the Louisiana Board of Regents. The NSLS is supported by the United States Department of Energy, Office of Science, Office of Basic Energy Sciences, under Contract No. DE-AC02-76CH00016. We thank Neil M. Boag for synthesizing samples of  $\text{Cu}(\text{CNdpm})_2$  and acknowledge the technical assistance of Ihor Ketsman and a number of helpful discussions with Neil Boag, Ihor Ketsman, and Evgeny Tsymbal.

## References and Notes

- (1) Zhu, X. Y. *Surf. Sci. Rep.* **2004**, *56*, 1.
- (2) Balaz, S.; Caruso, A. N.; Platt, N. P.; Dimov, D. I.; Boag, N. M.; Brand, J. I.; Losovyj, Ya. B.; Dowben, P. A. *J. Phys. Chem. B* **2007**, *111*, 7009–7016.
- (3) L'ovov, V. S.; Naaman, R.; Tiberkevich, V.; Vager, Z. *Chem. Phys. Lett.* **2003**, *381*, 650.
- (4) Cahen, D.; Naaman, R.; Vager, Z. *Adv. Funct. Mater.* **2005**, *15*, 1571.
- (5) Sabirianov, R. F.; Mei, W. N.; Lu, J.; Gao, Y.; Zeng, X. C.; Bolskar, R. D.; Jeppson, P.; Wu, N.; Caruso, A. N.; Dowben, P. A. *J. Phys.: Condens. Matter* **2007**, *19*, 082201.
- (6) Ishii, H.; Sugiyama, K.; Ito, E.; Seki, K. *Adv. Mater.* **1999**, *11*, 605.
- (7) Schwieger, T.; Peisert, H.; Knupfer, M. *Chem. Phys. Lett.* **2004**, *384*, 197–202.
- (8) Yamane, H.; Yabuuchi, Y.; Fukagawa, H.; Kera, S.; Okudaira, K. K.; Ueno, N. *J. Appl. Phys.* **2006**, *99*, 093705.
- (9) Ellis, T. S.; Park, K. T.; Ulrich, M. D.; Hulbert, S. L.; Rowe, J. E. *J. Appl. Phys.* **2006**, *100*, 093515.
- (10) Berner, S.; de Wild, M.; Ramoino, L.; Ivan, S.; Baratoff, A.; Güntherodt, H.-J.; Suzuki, H.; Schlettwein, D.; Jung, T. A. *Phys. Rev. B* **2003**, *68*, 115410.
- (11) Lu, X.; Hipps, K. W.; Wang, X. D.; Mazur, U. *J. Am. Chem. Soc.* **1996**, *118*, 7197.
- (12) Fukagawa, H.; Yamane, H.; Kera, S.; Okudaira, K. K.; Ueno, N. *Phys. Rev. B* **2006**, *73*, 041302(R).



- (13) Yamane, H.; Honda, H.; Fukagawa, H.; Ohya, M.; Hinuma, Y.; Kera, S.; Okudaira, K. K.; Ueno, N. *J. Electron Spectrosc. Relat. Phenom.* **2004**, *137*, 223.
- (14) Lukaszczuk, T.; Flechtner, K.; Merte, L. R.; Jux, N.; Maier, F.; Gottfried, J. M.; Steinhilber, H. P. *J. Phys. Chem. C* **2007**, *111*, 3090.
- (15) Kera, S.; Yabuuchi, Y.; Yamane, H.; Setoyama, H.; Okudaira, K. K.; Kahn, A.; Ueno, N. *Phys. Rev. B* **2004**, *70*, 085304.
- (16) Gorgoi, M.; Zahn, D. R. T. *J. Phys. IV* **2006**, *132*, 337.
- (17) Suzuki, T.; Kurahashi, M.; Yamauchi, Y. *J. Phys. Chem. B* **2002**, *106*, 7643–7646.
- (18) Suzuki, T.; Kurahashi, M.; Ju, X.; Yamauchi, Y. *J. Phys. Chem. B* **2002**, *106*, 11553.
- (19) Mathon, J. *J. Phys. F: Met. Phys.* **1986**, *16*, L217.
- (20) Mathon, J. *J. Phys. F: Met. Phys.* **1986**, *16*, 669.
- (21) Mathon, J.; Bergmann, G. *J. Phys. F: Met. Phys.* **1986**, *16*, 887.
- (22) Binder, K.; Hohenberg, P. C. *Phys. Rev. B* **1972**, *6*, 3461.
- (23) Edwards, D. M.; Mathon, J.; Wohlfarth, E. P. *J. Phys. F: Met. Phys.* **1973**, *3*, 161.
- (24) Edwards, D. M.; Mathon, J.; Wohlfarth, E. P. *J. Phys. F: Met. Phys.* **1975**, *5*, 1619.
- (25) Coutinho, S.; Edwards, D. M.; Mathon, J. *J. Phys. F: Met. Phys.* **1983**, *13*, L143.
- (26) Camley, R. E. *Phys. Rev. B* **1987**, *35*, 3608.
- (27) Fishman, F.; Schwabl, F.; Schwenk, D. *Phys. Lett. A* **1987**, *121*, 192.
- (28) Schwenk, D.; Fishman, F.; Schwabl, F. *Phys. Rev. B* **1988**, *38*, 11618.
- (29) Gradmann, U.; Bergholz, R. *Phys. Rev. Lett.* **1984**, *52*, 771.
- (30) Zheng, Y.; Lin, D. L.; Che, H. *Chin. J. Phys.* **1995**, *33*, 197.
- (31) Dowben, P. A.; LaGraffe, D.; Li, D.; Miller, A.; Zhang, L.; Dottle, L.; Onellion, M. *Phys. Rev. B* **1991**, *43*, 3171.
- (32) Lifshitz, E. M.; Pitaevski, L. P. *Statistical Physics, Part 2*; Pergamon: Oxford, U.K., 1980.
- (33) Peisert, H.; Schwiager, T.; Auerhammer, J. M.; Knupfer, M.; Golden, M. S.; Fink, J. *J. Appl. Phys.* **2001**, *90*, 466.
- (34) Okudaira, K. K.; Hasegawa, S.; Ishii, H.; Seki, K.; Harada, Y.; Ueno, N. *J. Appl. Phys.* **1999**, *85*, 6453–6461.
- (35) Lu, X.; Hipps, K. W.; Wang, X. D.; Mazur, U. *J. Am. Chem. Soc.* **1996**, *118*, 7197–7202.
- (36) Xiao, J.; Sokolov, A.; Dowben, P. A. *Appl. Phys. Lett.* **2007**, *90*, 242907.
- (37) Dowben, P. A.; Xiao, J.; Xu, B.; Sokolov, A.; Doudin, B. *Appl. Surf. Sci.* **2008**, *254*, 4238–4244.
- (38) Liu, J.; Xiao, J.; Choi, S.-B.; Jeppson, P.; Jarabek, L.; Losovyj, Ya. B.; Caruso, A. N.; Dowben, P. A. *J. Phys. Chem. B* **2006**, *110*, 26180–26184.
- (39) Sugiyama, T.; Sasaki, T.; Kera, S.; Ueno, N.; Munakata, T. *Appl. Phys. Lett.* **2006**, *89*, 202116.
- (40) Weber-Bargioni, A.; Auwarter, W.; Klappenberger, F.; Reichert, J.; Lefrançois, S.; Strunskus, T.; Wöll, C.; Schiffrin, A.; Pennek, Y.; Barth, J. V. *ChemPhysChem* **2008**, *9*, 89–94.
- (41) Velev, J. P.; Dowben, P. A.; Tsymbl, E. Y.; Jenkins, S. J.; Caruso, A. N. *Surf. Sci. Rep.*, in press.
- (42) Wisbey, D.; Feng, D.; Bremer, M. T.; Borca, C. N.; Caruso, A. N.; Silvernail, C. M.; Belot, J.; Vescovo, E.; Ranno, L.; Dowben, P. A. *J. Am. Chem. Soc.* **2007**, *129*, 6249–6254.
- (43) Silvernail, C. M.; Yap, G.; Sommer, R. D.; Rheingold, A. L.; Day, V. W.; Belot, J. A. *Polyhedron* **2001**, *20*, 3113.
- (44) (a) Vescovo, E.; Kim, H.-J.; Dong, Q.-Y.; Nintzel, G.; Carlson, D.; Hulbert, S.; Smith, N. V. *Synchrotron Radiat. News* **1999**, *12*, 10. (b) Johnson, P. D.; Brooks, N. B.; Hulbert, S. L.; Klaffy, R.; Clarke, A.; Sinković, B.; Smith, N. V.; Celotta, R.; Kelly, M. H.; Pierce, D. T.; Sheinfein, M. R.; Waclawski, B. J.; Howells, M. R. *Rev. Sci. Instrum.* **1992**, *63*, 1902.
- (45) Dowben, P. A.; Waldfried, C.; Komesu, T.; Welipitiya, D.; McAvoy, T.; Vescovo, E. *Chem. Phys. Lett.* **1998**, *283*, 44–50.
- (46) Losovyj, Y.; Ketsman, I.; Morikawa, E.; Wang, Z.; Tang, J.; Dowben, P. *Nucl. Instrum. Methods Phys. Res., Sect. A* **2007**, *582*, 264.
- (47) Dowben, P. A.; LaGraffe, D.; Onellion, M. *J. Phys.: Condens. Matter* **1989**, *1*, 6571.
- (48) Hormes, J.; Scott, J. D.; Suller, V. P. *Synchrotron Radiat. News* **2006**, *19*, 27.
- (49) Johnson, P. D. *Rep. Prog. Phys.* **1997**, *60*, 1217–1304.
- (50) Choi, J.; Dowben, P. A. *Surf. Sci.* **2006**, *600*, 2997–3002.
- (51) Chen, Q.; Onellion, M.; Wall, A.; Dowben, P. A. *J. Phys.: Condens. Matter* **1992**, *4*, 7985–7996.
- (52) (a) Alkemper, U.; Carbone, C.; Vescovo, E.; Eberhardt, W.; Rader, O.; Gudat, W. *Phys. Rev. B* **1994**, *50*, 17496. (b) Vescovo, E.; Carbone, C.; Alkemper, U.; Rader, O.; Kachel, T.; Gudat, W.; Eberhardt, W. *Phys. Rev. B* **1995**, *52*, 13497. (c) Izquierdo, J.; Vega, A.; Balbás, L. C. *Surf. Sci.* **1996**, *352–354*, 902–906. (d) Schneider, C. M.; de Miguel, J. J.; Bressler, P.; Schuster, P.; Miranda, R.; Kirschner, J. *J. Electron Spectrosc. Relat. Phenom.* **1990**, *51*, 263. (e) Yu, D. H.; Donath, M.; Braun, J. *Phys. Rev. B* **2003**, *68*, 155415.
- (53) Wisbey, D.; Wu, Ning; Caruso, A. N.; Belot, J.; Losovyj, Ya. B.; Vescovo, E.; Dowben, P. A. Manuscript in preparation.
- (54) Stewart, J. J. P. PM3. *Encyclopedia of Computational Chemistry*; Wiley: New York, 1998.
- (55) Feng, D.-Q.; Wisbey, D.; Tai, Y.; Losovyj, Ya. B.; Zharnikov, M.; Dowben, P. A. *J. Phys. Chem. B* **2006**, *110*, 1095.
- (56) Xiao, J.; Poulsen, M.; Reddy, S.; Takacs, J. M.; Losovyj, Ya. B.; Dowben, P. A. *Polym. Sci. Eng.* **2008**, in press.
- (57) Muscat, J.; Wander, A.; Harrison, N. M. *Chem. Phys. Lett.* **2001**, *342*, 397.
- (58) Perger, W. F. *Chem. Phys. Lett.* **2003**, *368*, 319.
- (59) Ortega, J. E.; Himpel, F. J.; Li, D.; Dowben, P. A. *Solid State Commun.* **1994**, *91*, 807–811.
- (60) Dowben, P. A. *Surf. Sci. Rep.* **2000**, *40*, 151–247.
- (61) Tanaka, A.; Takeda, Y.; Imamura, M.; Sato, S. *Appl. Surf. Sci.* **2004**, *237*, 537–542.
- (62) Hövel, H.; Grimm, B.; Pollmann, M.; Reihl, B. *Phys. Rev. Lett.* **1998**, *81*, 4608–4611.
- (63) Amsalem, P.; Giovannelli, L.; Themlin, J. M.; Koudia, M.; Abel, M.; Oison, V.; Ksari, Y.; Mossayan, M.; Porte, L. *Surf. Sci.* **2007**, *601*, 4185–4188.
- (64) Lu, X. H.; Grobis, M.; Khoo, K. H.; Louie, S. G.; Crommie, M. F. *Phys. Rev. B* **2004**, *70*, 115418.
- (65) Neaton, J. B.; Hybertsen, M. S.; Louie, S. G. *Phys. Rev. Lett.* **2006**, *97*, 216405.
- (66) Schiller, F.; Ruiz-Osés, M.; Ortega, J. E.; Segovia, P.; Martínez-Blanco, J.; Doyle, B. P.; Pérez-Dieste, V.; Lobo, J.; Néel, N.; Berndt, R.; Kröger, J. *J. Chem. Phys.* **2006**, *125*, 144719.
- (67) Feng, D.-Q.; Wisbey, D.; Tai, Y.; Losovyj, Ya. B.; Zharnikov, M.; Dowben, P. A. *J. Phys. Chem. B* **2006**, *110*, 1095–1098.
- (68) Feng, D.-Q.; Caruso, A. N.; Schulz, D. L.; Losovyj, Ya. B.; Dowben, P. A. *J. Phys. Chem. B* **2005**, *109*, 16382–16389.
- (69) Kilian, L.; Hauschild, A.; Temirov, R.; Soubatch, S.; Schöll, A.; Bendounan, A.; Reinert, F.; Lee, T.-L.; Tautz, F. S.; Sokolowski, M.; Umbach, E. *Phys. Rev. Lett.* **2008**, *100*, 136103.
- (70) (a) Dowben, P. A.; Choi, J.; Morikawa, E.; Xu, Bo. The Band Structure and Orientation of Molecular Adsorbates on Surfaces by Angle-Resolved Electron Spectroscopies In *Handbook of Thin Films. Volume 2: Characterization and Spectroscopy of Thin Films*; Nalwa, H. S., Ed.; Academic Press: New York, 2002; pp 61–114. (b) Plummer, E. W.; Eberhardt, W. *Adv. Chem. Phys.* **1982**, *49*, 533.
- (71) (a) Carbone, C.; Vescovo, E.; Kläsger, R.; Eberhardt, W.; Rader, O.; Gudat, W. *J. Appl. Phys.* **1994**, *76*, 6966. (b) Kläsger, R.; Schmitz, D.; Carbone, C.; Eberhardt, W.; Lang, P.; Zeller, R.; Dederichs, P. H. *Phys. Rev. B* **1998**, *57*, R696. (c) Garrison, K.; Chang, Y.; Johnson, P. D. *Phys. Rev. Lett.* **1993**, *71*, 2801.
- (72) Duan, C.-G.; Jaswal, S. S.; Tsymabl, E. Y. *Phys. Rev. Lett.* **2006**, *97*, 047201.
- (73) Oleinik, I. I.; Tsymabl, E. Y.; Pettifor, E. Y. *Phys. Rev. B* **2001**, *65*, 02040.
- (74) (a) Getzlaff, M.; Cherepkov, N. A.; Schönhense, G. *Phys. Rev. B* **1995**, *52*, 3421. (b) Getzlaff, M.; Bansmann, J.; Schönhense, G. *Phys. Rev. Lett.* **1993**, *71*, 793.
- (75) (a) Alexander, S. *Solid State Commun.* **1966**, *4*, 115. (b) Astrov, D. N. *Sov. Phys. JETP USSR* **1960**, *11*, 708. (c) Hornreich, R. *Phys. Rev.* **1967**, *161*, 506. (d) Fiebig, M. *J. Phys. D: Appl. Phys.* **2005**, *38*, R123–R152. (e) Spaldin, N. A.; Fiebig, M. *Science* **2005**, *309*, 391–392. (f) Duan, C.-G.; Jaswal, S. S.; Tsymabl, E. Y. *Phys. Rev. Lett.* **2006**, *97*, 047201. (g) Weisheit, M.; Fähler, S.; Marty, A.; Souche, Y.; Poinsignon, C.; Givord, D. *Science* **2007**, *315*, 349–351. (h) Erenstein, W.; Wiora, M.; Prieto, J. L.; Scott, J. F.; Mathur, N. D. *Nat. Mater.* **2007**, *6*, 348–351. (i) Borisov, P.; Hochstrat, A.; Chen, X.; Kleemann, W.; Binek, Ch. *Phys. Rev. Lett.* **2005**, *94*, 117203. (j) Binek, Ch.; Doudin, B. *J. Phys.: Condens. Matter* **2005**, *17*, L39.